International Journal of Engineering Inventions
e-ISSN: 2278-7461, p-ISSN: 2319-6491
Volume 15, Issue 8 [August 2026] PP: 42-51

Super-Twisting Sliding Mode Control for Robust DC Motor Speed Regulation under Load Disturbances and Parameter Uncertainties

Dao Thi My Linh[1], Nguyen Thi Xuan Mai[2], Tran Minh Hai[1*]
[1]*Faculty of Technology and Engineering, Thai Binh University*
[2]*Thai Nguyen University of Technology*

Abstract
This paper presents a comparative study of three speed-control strategies—proportional–integral–derivative (PID) control, conventional Sliding Mode Control (SMC), and Super-Twisting Sliding Mode Control (STSMC)—for a direct-current (DC) motor drive subject to load disturbances and parameter uncertainties. The study focuses on the tradeoff among tracking performance, disturbance rejection, chattering, and control effort rather than on speed response alone. The STSMC is developed from the super-twisting algorithm, and its control parameters are selected through a constrained search procedure to preserve disturbance-rejection capability while limiting control-signal oscillations. The three controllers are evaluated on the same motor model, under the same voltage constraint, for nominal operation, load-torque disturbance, parameter uncertainty, and combined uncertainty–disturbance scenarios. Simulation results show that PID provides the fastest nominal transient response, whereas conventional SMC yields the smallest peak speed deviation under a nominal load disturbance. STSMC provides a more favorable robustness–smoothness compromise: relative to conventional SMC, the post-disturbance total variation of the control signal is reduced by approximately 82.0%, and the RMS value of the control-voltage increments is reduced by approximately 84.4%. Under simultaneous parameter uncertainty and load disturbance, STSMC reduces the IAE and ITAE by approximately 80.6% and 97.6%, respectively, relative to SMC, while substantially reducing actuator saturation. These results indicate that STSMC is a suitable solution when speed tracking, robustness, and control-signal smoothness must be considered simultaneously.
Index Terms—DC motor, sliding mode control, super-twisting sliding mode control, PID control, disturbance rejection, chattering, robust control.

Date of Submission: 15-08-2026 Date of acceptance: 30-08-2026

I. INTRODUCTION

Direct-current (DC) motors remain widely used in electric-drive applications because of their relatively simple structure, favorable torque characteristics, and wide speed-regulation range [1], [2]. In applications such as robotics, actuators, automated systems, and precision drives, speed-control performance directly affects system accuracy and overall efficiency. In practical operation, however, DC motors are subject to load-torque disturbances, actuator-voltage limitations, and variations in electromechanical parameters, all of which can degrade tracking performance and closed-loop dynamics [3], [4].

Proportional–integral–derivative (PID) control is widely used for DC motor speed regulation because of its simple structure, ease of tuning, and straightforward implementation [2], [5], [6]. Under operating conditions close to the nominal point, PID can provide a fast transient response and a small steady-state error. Its performance, however, depends strongly on the selected gains and plant dynamics; therefore, load variations or parameter deviations from their design values may deteriorate disturbance rejection and tracking performance [4]–[6].

Sliding Mode Control (SMC) is a nonlinear control technique that is well known for its robustness against certain classes of disturbances and parameter uncertainties [7]–[10]. By driving the system trajectory toward an appropriately designed sliding manifold, SMC can preserve satisfactory tracking performance under varying operating conditions. Nevertheless, the discontinuous switching action of conventional SMC generally induces chattering, which increases control-signal oscillations and actuator activity [9]–[11]. Higher-order sliding-mode approaches, particularly Super-Twisting Sliding Mode Control (STSMC), have therefore been developed to retain the robustness properties of sliding-mode control while reducing direct discontinuities in the control signal [10], [11], [15]–[19].

Recent studies have extended SMC and its higher-order variants to electrical-drive systems. Rauf et al. [12] developed continuous dynamic sliding-mode control for a converter-fed DC motor with mismatched disturbances; Zhou et al. [13] proposed a continuous adaptive terminal sliding-mode structure for DC motor control; and Ma'arif and Çakan [14] reported both simulation and hardware implementation of SMC for a DC motor. For super-twisting control, the studies in [15]–[19] demonstrated chattering reduction, improved speed tracking, and enhanced disturbance rejection in electrical drives. However, a unified comparison of PID, conventional SMC, and STSMC on the same DC motor model, with simultaneous quantification of tracking performance, disturbance rejection, chattering, control effort, and actuator saturation, remains insufficiently addressed.

Motivated by these considerations, this study develops and compares PID, conventional SMC, and STSMC for the same DC motor model under load disturbance, parameter uncertainty, and voltage constraints. Rather than considering tracking error alone, four performance aspects are evaluated simultaneously: tracking performance, disturbance rejection, chattering, and control effort. The STSMC parameters are selected through a constrained search procedure to balance disturbance rejection against control-signal smoothness. To ensure a meaningful robustness assessment, the actual plant parameters are varied while all controllers retain their nominal design model.

The main contributions of this study are as follows: a unified comparison framework is established for PID, SMC, and STSMC under identical operating conditions; an STSMC law is designed for DC motor speed tracking and the convergence condition of the sliding variable is analyzed; and the tradeoff among tracking performance, disturbance rejection, chattering, and control effort is quantified using transient indices, IAE, ITAE, control-signal total variation, and actuator saturation. The study therefore clarifies whether STSMC can preserve the robustness characteristics of conventional SMC while improving control smoothness and practical implementability.

The remainder of this paper is organized as follows. Section II presents the DC motor dynamics, disturbance model, parameter uncertainties, and control problem formulation. Section III develops the PID, SMC, and STSMC controllers together with the convergence analysis. Section IV presents the simulation setup, comparative results, and discussion. Section V concludes the paper.

II. DC MOTOR MODEL AND PROBLEM FORMULATION

This section establishes the electromechanical model of the DC motor, describes the load disturbance and parameter uncertainties, and defines the assumptions and control objectives common to the PID, conventional SMC, and Super-Twisting Sliding Mode Control (STSMC) structures. Using a common model and identical physical constraints provides a consistent basis for the controller comparisons presented in the following sections.

2.1. Dynamic Model of the DC Motor

Consider a separately excited DC motor, in which the armature voltage u(t) is the control input, the armature current and rotor angular speed ω(t) are the state variables, and the load torque is treated as an external disturbance. The standard motor model is obtained from the electrical and mechanical equations [1].
According to Kirchhoff's voltage law, the armature-circuit equation is written as

$$u(t) = R_a i_a(t) + L_a \frac{di_a(t)}{dt} + K_e \omega(t) \tag{1}$$

where R_a and L_a denote the armature resistance and inductance, respectively, and K_e is the back-EMF constant. The electromagnetic torque generated by the motor is proportional to the armature current:

$$T_e(t) = K_t i_a(t) \tag{2}$$

where K_t is the torque constant. The torque-balance equation on the rotor shaft is given by

$$J \frac{d\omega(t)}{dt} = K_t i_a(t) - B\omega(t) - T_L(t) \tag{3}$$

where J is the equivalent rotor inertia and B is the viscous-friction coefficient. From (1)–(3), the differential model of the motor is expressed as

$$i_a(t) = -\frac{R_a}{L_a} i_a(t) - \frac{K_e}{L_a}\omega(t) + \frac{1}{L_a}u(t) \tag{4}$$

and

$$\dot{\omega}(t) = \frac{K_t}{J} i_a(t) - \frac{B}{J}\omega(t) - \frac{1}{J}T_L(t) \tag{5}$$

Define the state vector as

$$x(t) = [i_a(t) \quad \omega(t)]^T \tag{6}$$

then the system can be represented in state-space form as

$$\dot{x}(t) = Ax(t) + B_u u(t) + B_d T_L(t) \tag{7}$$

with

$$A = \begin{bmatrix} -\frac{R_a}{L_a} & -\frac{K_e}{L_a} \\ \frac{K_t}{J} & -\frac{B}{J} \end{bmatrix}, \quad B_u = \begin{bmatrix} \frac{1}{L_a} \\ 0 \end{bmatrix}, \quad B_d = \begin{bmatrix} 0 \\ -\frac{1}{J} \end{bmatrix} \tag{8}$$

and the controlled output is the rotor speed

$$y(t) = \omega(t) = [0 \quad 1]x(t) \tag{9}$$

Equations (4)–(5) show that the armature voltage u(t) acts directly on the current dynamics but does not appear explicitly in the first derivative of the rotor speed. Hence, the relative degree from armature voltage to rotor speed is two. This property motivates the use of a sliding variable containing the derivative of the tracking error in the SMC and STSMC designs.

2.2. Load Disturbance, Parameter Uncertainty, and Actuator Constraint

In practical operation, control performance is affected simultaneously by load-torque variations and parameter deviations. The load torque is represented in the general form

$$T_L(t) = T_{L0} + \Delta T_L(t) \tag{10}$$

where the first term denotes the nominal load and the second term represents its time-varying component. To evaluate disturbance rejection while preserving a bounded disturbance rate, the simulation employs a smooth load transition of the form

$$T_L(t) = \frac{T_d}{2}\left[1 + \tanh[\alpha(t - t_d)]\right] \tag{11}$$

where T_d is the load magnitude, t_d is the application time, and $\alpha>0$ determines the transition slope. For sufficiently large α, (11) approximates a step load while avoiding the unbounded ideal derivative at the switching instant, which is more consistent with the assumptions commonly adopted in STSMC analysis [10], [11].

Parameter uncertainty is modeled in relative form as

$$p = p_0(1 + \delta_p), \qquad |\delta_p| \le \bar{\delta}_p \tag{12}$$

where p_0 denotes the nominal value, δ_p is the relative deviation, and $\bar{\delta}_p$ is its known bound. In this study, R_a, J, and B are selected for the robustness analysis because they directly reflect the effects of winding-temperature variation and changes in the mechanical load characteristics. The final uncertainty scenario is defined by

$$R_a' = 1.3R_a, J' = 1.5J, B' = 1.4B \tag{13}$$

In all test cases, the controllers retain the nominal parameter values. This setting ensures that the uncertainty test evaluates the intrinsic robustness of the control laws rather than inadvertently providing the controllers with the perturbed plant parameters.

The control voltage is limited by the power converter capability:

$$|u(t)| \le U_{\max} \tag{14}$$

This constraint is applied uniformly to PID, SMC, and STSMC. Consequently, in addition to tracking quality, the degree of voltage saturation provides an indication of actuator demand.

2.3. Control Problem Formulation and Assumptions

The speed-tracking error is defined consistently throughout this study as

$$e(t) = \omega(t) - \omega_{\text{ref}}(t) \tag{15}$$

The reference speed is constant in the simulation experiments; therefore,

$$\omega_{\text{ref}} = 80 \text{ rad s}^{-1}, \qquad \dot{\omega}_{\text{ref}} = \ddot{\omega}_{\text{ref}} = 0 \tag{16}$$

The control objective is to design u(t) such that the closed-loop system remains stable and the tracking error converges to zero under nominal conditions, while remaining small in the presence of disturbances, parameter uncertainties, and the actuator-voltage constraint:

$$e(t) \to 0, t \to \infty \tag{17}$$

To establish the convergence condition of the super-twisting algorithm, the load disturbance and model mismatch are mapped into the sliding-variable dynamics in Section III. The resulting equivalent perturbation is denoted by $\Delta(t)$ and is assumed to have a bounded rate of variation:

$$|\dot{\Delta}(t)| \le L, 0 < L < \infty \tag{18}$$

In addition, all physical motor parameters are assumed positive and bounded within known intervals, while the armature current and rotor speed are assumed measurable. To avoid using the unknown load torque directly in the control law, the speed derivative is not computed from the mechanical equation containing the load torque; instead, it is estimated using a first-order filtered differentiator

$$\widehat{\dot{\omega}}(s) = \frac{s}{\tau_D s + 1}\, \omega(s) \tag{19}$$

where $\tau_d > 0$ is the filter time constant. This structure attenuates measurement-noise amplification relative to ideal numerical differentiation and ensures that the controller does not require direct knowledge of the load torque. Based on the above model, constraints, and assumptions, Section III develops the PID, conventional SMC, and STSMC controllers and establishes the corresponding stability and convergence conditions.

III. CONTROLLER DESIGN

This section develops the three controllers using the same DC motor model introduced in Section II. PID is used as the benchmark controller, conventional SMC serves as the sliding-mode baseline, and STSMC is the proposed approach intended to preserve the robustness of SMC while reducing switching-induced control oscillations. The speed-tracking error is defined consistently as

$$e(t) = \omega(t) - \omega_{\mathrm{ref}}(t). \tag{20}$$

3.1. Benchmark PID Controller

The PID controller is adopted as a benchmark because of its simple structure and widespread use in electric-drive systems [2], [5], [6]. The control signal is defined as

$$u_{\mathrm{PID}}(t) = -K_p e(t) - K_i \int_0^t e(\tau)\, d\tau - K_d \dot{e}(t), \tag{21}$$

where K_p, K_i, and K_d are the proportional, integral, and derivative gains, respectively. The negative sign follows from the error definition in (20). To account for the voltage limitation of the power converter, the actual control signal is constrained by

$$u_{\mathrm{PID,act}} = \mathrm{sat}_{U_{\max}}(u_{\mathrm{PID}}), \tag{22}$$

with

$$\mathrm{sat}_{U_{\max}}(u) = \begin{cases} U_{\max}, & u > U_{\max}, \\ u, & |u| \le U_{\max}, \\ -U_{\max}, & u < -U_{\max}. \end{cases} \tag{23}$$

In the simulations, conditional anti-windup is applied to prevent excessive accumulation of the integral term during actuator saturation. The PID gains are kept fixed in all investigated scenarios.

3.2. Conventional Sliding Mode Controller

From the motor mechanical model, the armature voltage does not appear explicitly in the first derivative of the rotor speed. Therefore, to match the relative degree from armature voltage to speed, the sliding surface is selected as [7]–[10]

$$s(t) = \dot{e}(t) + \lambda e(t), \qquad \lambda > 0. \tag{24}$$

When the system reaches the sliding regime, $s = 0$, the error dynamics satisfy

$$\dot{e}(t) + \lambda e(t) = 0, \tag{25}$$

and hence

$$e(t) = e(t_s) e^{-\lambda(t - t_s)}, \qquad t \ge t_s, \tag{26}$$

where t_s denotes the time at which the trajectory reaches the sliding manifold. Since $\lambda > 0$, the tracking error converges to zero after the sliding regime is established. Differentiating the sliding surface and using the motor model in Section II gives

$$\dot{s} = F(x,t) + Gu + d(t), \tag{27}$$

where

$$G = \frac{K_t}{J L_a} > 0, \tag{28}$$

and, for the nominal model,

$$F(x,t) = -\frac{K_t R_a}{J L_a} i_a - \frac{K_t K_e}{J L_a} \omega + \left(\lambda - \frac{B}{J}\right) \dot{\omega} - \lambda \dot{\omega}_{\mathrm{ref}} - \ddot{\omega}_{\mathrm{ref}}, \tag{29}$$

where $d(t)$ represents the equivalent disturbance and model deviations mapped into the sliding-variable dynamics. Neglecting the perturbation in the nominal model and imposing $\dot{s} = 0$, the equivalent control component is obtained as

$$u_{\mathrm{eq}} = -\frac{F(x,t)}{G}. \tag{30}$$

Expanding the expression in terms of the physical motor variables gives

$$u_{\mathrm{eq}} = R_a i_a + K_e \omega - \frac{J L_a}{K_t}\left[\left(\lambda - \frac{B}{J}\right)\dot{\omega} - \lambda \dot{\omega}_{\mathrm{ref}} - \ddot{\omega}_{\mathrm{ref}}\right]. \tag{31}$$

For a constant speed reference, $\dot{\omega}_{\mathrm{ref}} = \ddot{\omega}_{\mathrm{ref}} = 0$; therefore,

$$u_{\mathrm{eq}} = R_a i_a + K_e \omega - \frac{J L_a}{K_t}\left(\lambda - \frac{B}{J}\right)\dot{\omega}. \tag{32}$$

The conventional SMC law is constructed as

$$u_{\mathrm{SMC}} = u_{\mathrm{eq}} - \frac{J L_a}{K_t} K_s \mathrm{sat}\left(\frac{s}{\phi}\right), \tag{33}$$

where $K_s > 0$ is the switching gain and $\phi > 0$ is the boundary-layer width. The saturation function is used in place of the sign function to mitigate chattering in practical implementation [9]–[11]. However, smoothing the switching component results in quasi-sliding motion in a neighborhood of the sliding manifold and introduces a tradeoff between tracking accuracy and control-signal oscillation.

3.3. Proposed Super-Twisting Sliding Mode Controller

To reduce the switching activity associated with first-order SMC while retaining disturbance-rejection capability, this study employs the super-twisting algorithm, a higher-order SMC method that provides finite-time convergence of the sliding variable under appropriate perturbation conditions [11]. Recent studies on electrical-drive systems have likewise shown that STSMC can reduce chattering while preserving tracking performance under disturbances and uncertainties [15]–[19]. The control law is written as

$$u_{\mathrm{STSMC}} = u_{\mathrm{eq}} + \frac{JL_a}{K_t} u_{\mathrm{ST}}, \tag{34}$$

where the super-twisting component is defined by

$$u_{\mathrm{ST}} = -k_1 |s|^{1/2} \mathrm{sat}\left(\frac{s}{\varepsilon}\right) + v, \tag{35}$$

and the auxiliary state v evolves according to

$$\dot{v} = -k_2 \mathrm{sat}\left(\frac{s}{\varepsilon}\right), \tag{36}$$

with $k_1 > 0$, $k_2 > 0$, and $\varepsilon > 0$. In the theoretical analysis, the saturation function is replaced by $\mathrm{sign}(s)$; the saturated form above is used in simulation to avoid ideal switching and improve numerical implementability.
Substituting the ideal STSMC law into the sliding-variable dynamics yields the reduced-order system

$$\dot{s} = -k_1 |s|^{1/2} \mathrm{sign}(s) + v + \Delta(t), \tag{37}$$

$$\dot{v} = -k_2 \mathrm{sign}(s), \tag{38}$$

where $\Delta(t)$ collects the mapped load disturbance, parameter uncertainty, and residual model mismatch. Compared with conventional SMC, the discontinuous action does not enter the control voltage directly but is introduced through higher-order dynamics, thereby substantially reducing control-signal oscillations around the sliding manifold.
The final signal applied to the actuator is constrained by

$$u_{\mathrm{act}} = \mathrm{sat}_{U_{\max}}(u_{\mathrm{STSMC}}). \tag{39}$$

3.4. Convergence and Stability Analysis of STSMC

Assume that the equivalent perturbation is differentiable almost everywhere and that its rate of variation is bounded by

$$\left|\dot{\Delta}(t)\right| \le L, \tag{40}$$

$L > 0$, with L_Δ finite. This is a standard assumption in super-twisting analysis and is consistent with physical disturbances having a finite rate of variation [11].
Define the transformed variables

$$\xi_1 = |s|^{1/2} \mathrm{sign}(s), \qquad \xi_2 = v + \Delta(t), \tag{41}$$

and

$$\xi = [\xi_1 \quad \xi_2]^T. \tag{42}$$

Consider the quadratic Lyapunov candidate

$$V(\xi) = \xi^T P \xi, \tag{43}$$

where $P = P^T > 0$. If the gains k_1 and k_2 are selected sufficiently large relative to the perturbation bound, there exist positive-definite matrices P and Q such that [11]

$$\dot{V} \le -\frac{1}{|\xi_1|} \xi^T Q \xi < 0, \qquad \xi \ne 0. \tag{44}$$

The above inequality guarantees that s and $\dot{s}$ converge to zero in finite time. When $s = 0$, the error dynamics reduce to (25), and hence $e(t) \to 0$. Therefore, under the stated perturbation assumptions and appropriate gain conditions, STSMC guarantees finite-time convergence to the sliding manifold and asymptotic convergence of the speed-tracking error.

3.5. Speed-Derivative Processing and Implementation-Parameter Selection

To avoid assuming direct knowledge of the load torque, the speed derivative is not computed from the mechanical equation containing T_L. Instead, a first-order filtered differentiator is employed

$$\tau_d \dot{\omega}_f + \omega_f = \omega, \tag{45}$$

and the speed-derivative estimate is obtained as

$$\widehat{\dot{\omega}} = \frac{\omega - \omega_f}{\tau_d}. \tag{46}$$

Accordingly, the sliding variable used in the implementable controller is constructed as

$$s = \left(\widehat{\dot{\omega}} - \dot{\omega}_{\mathrm{ref}}\right) + \lambda(\omega - \omega_{\mathrm{ref}}). \tag{47}$$

This structure clearly separates the actual plant model from the nominal model used by the controller. Consequently, the parameter-uncertainty scenarios in Section IV represent a genuine robustness test: the plant parameters vary while the controller parameters remain fixed. The gains k_1, k_2, and ε are selected through a constrained search procedure to balance disturbance rejection, chattering, control energy, and actuator saturation; the final parameter set is reported in the simulation setup.

IV. SIMULATION RESULTS AND DISCUSSION

4.1. Simulation Setup

The PID, conventional SMC, and STSMC controllers were evaluated using the same DC motor model, initial conditions, and actuator-voltage constraint to ensure a consistent comparison. The reference speed was fixed at $\omega_{ref} = 80(\mathrm{rad/s})$ and the armature voltage was constrained by $|u(t)| \leq 24\mathrm{V}$. The load-torque disturbance was selected as $T_L = 0.15\mathrm{N} \cdot \mathrm{m}$, and was applied at $t = 6\mathrm{s}$. For the uncertainty scenario, $R_a = 1.3R_{a0}$, $J = 1.5J_0$, and $B = 1.4B_0$ were used, while all controllers retained the nominal model parameters.

The benchmark-controller parameters were fixed as follows: PID used $K_p = 3.7$, $K_i = 6.4$, $K_d = 0.55$; conventional SMC used $\lambda = 10$, $K = 220$, and $\varphi = 3$. The optimized STSMC parameters were selected as $\lambda = 10, k_1 = 12, k_2 = 8, \varepsilon = 0.025$

The selected parameters satisfy the closed-loop stability requirement and the actuator-voltage constraint for all investigated scenarios.

4.2. Nominal Speed-Tracking Performance

Fig. 1 shows that PID provides the fastest nominal response, although a small overshoot is observed. Conventional SMC nearly eliminates overshoot, whereas STSMC exhibits transient behavior comparable to SMC with a slightly shorter rise time. The corresponding quantitative indices are summarized in Table I.

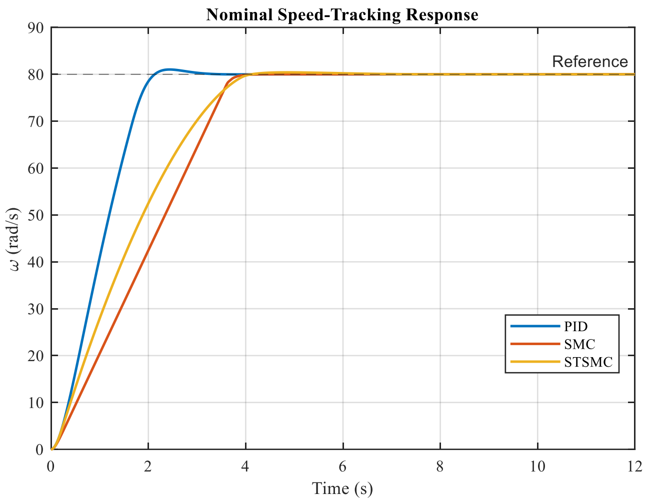

Fig. 1. Nominal speed-tracking responses of the DC motor under PID, conventional SMC, and STSMC.

4.3. Load-Disturbance Rejection

Fig. 2 shows that PID is most affected by the load variation; conventional SMC yields the smallest instantaneous speed deviation, whereas STSMC still maintains a substantially smaller deviation than PID. Specifically, STSMC reduces the maximum speed deviation by approximately 79.4% relative to PID.

Fig. 3 confirms the same trend in the tracking error. The IAE, ITAE, and recovery-time indices in Table I show that conventional SMC provides the strongest nominal disturbance rejection, whereas STSMC maintains satisfactory tracking performance with a considerably smoother control signal.

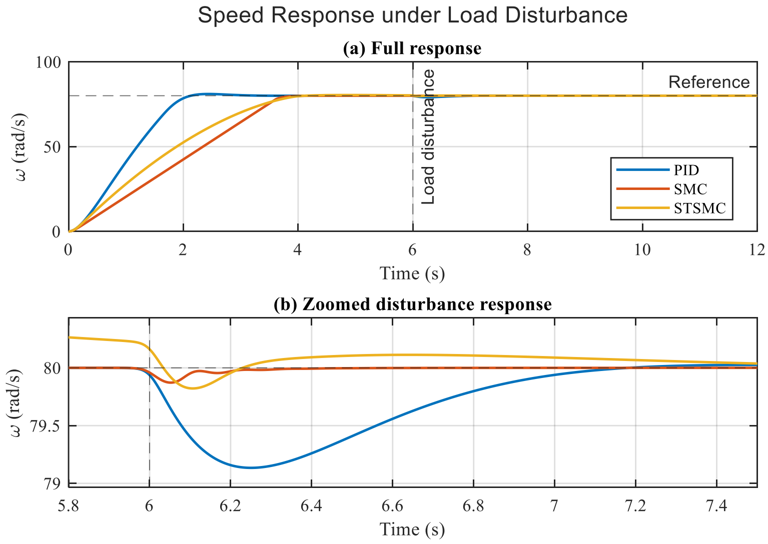

Fig. 2. Speed responses under load-torque disturbance: (a) complete responses and (b) enlarged disturbance transient.

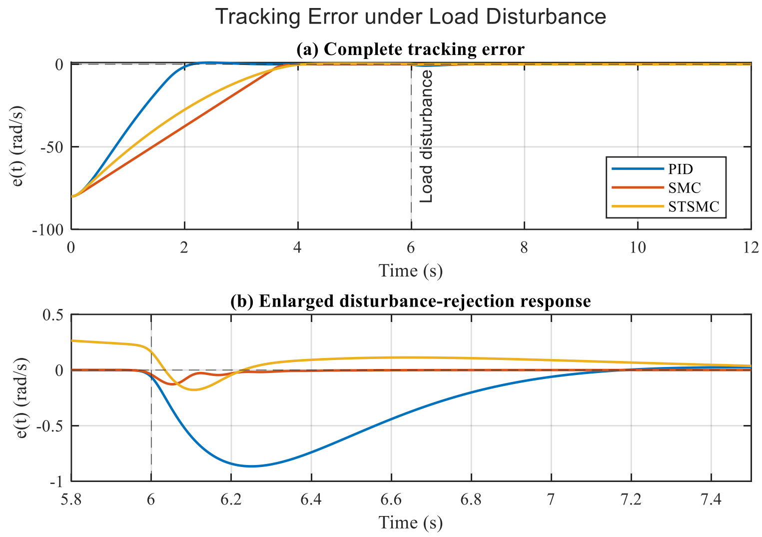

Fig. 3. Speed-tracking errors under load-torque disturbance: (a) complete responses and (b) enlarged disturbance-rejection responses.

4.4. Sliding Dynamics and Chattering Reduction

Fig. 4 shows that both conventional SMC and STSMC drive the sliding variable toward the vicinity of $s = 0$ and recover after the disturbance is applied. For STSMC, the final value of the sliding variable is $|s(t_f)| = 4.01 \times 10^{-4}$ indicating that the trajectory remains within a very small neighborhood of the sliding manifold.

The most pronounced difference appears in the control signal shown in Fig. 5. Relative to conventional SMC, STSMC reduces the post-disturbance total variation by approximately 82.0% and the RMS of the voltage increments by approximately 84.4%. These results confirm that STSMC effectively suppresses chattering without compromising closed-loop tracking stability.

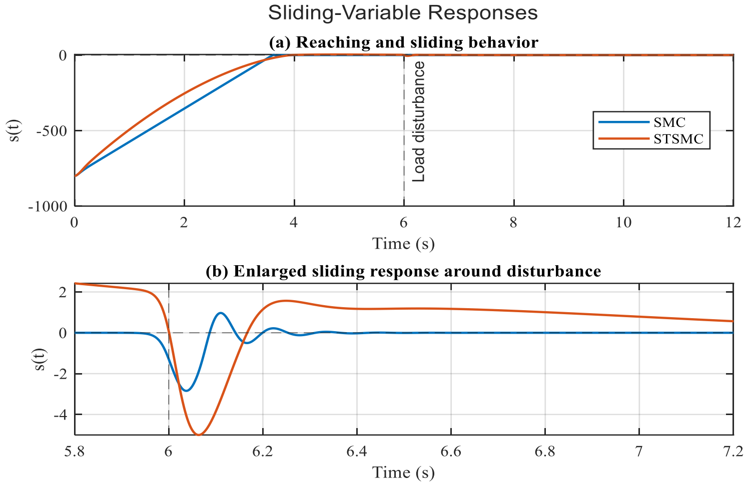

Fig. 4. Sliding-variable responses of conventional SMC and STSMC: (a) reaching and sliding behavior and (b) enlarged response around the load disturbance.

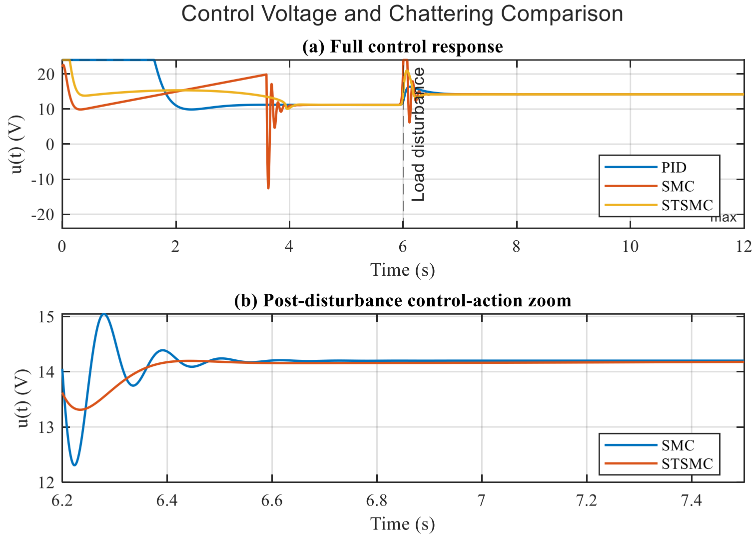

Fig. 5. Control-voltage responses: (a) complete control actions and (b) enlarged post-disturbance responses highlighting the reduction in control-signal oscillations achieved by STSMC.

4.5. Robustness under Parameter Uncertainty

Fig. 6 presents the combined parameter-uncertainty and load-disturbance case, while all controllers retain their nominal design parameters. All three methods preserve closed-loop stability and eventually recover the reference speed. Under this scenario, STSMC reduces IAE and ITAE by approximately 80.6% and 97.6%, respectively, relative to conventional SMC, indicating a substantially lower accumulated tracking error under combined uncertainty. The saturation ratio of STSMC is only 3.333%, which is markedly lower than those of the two benchmark controllers; the complete performance indices are summarized in Table II.

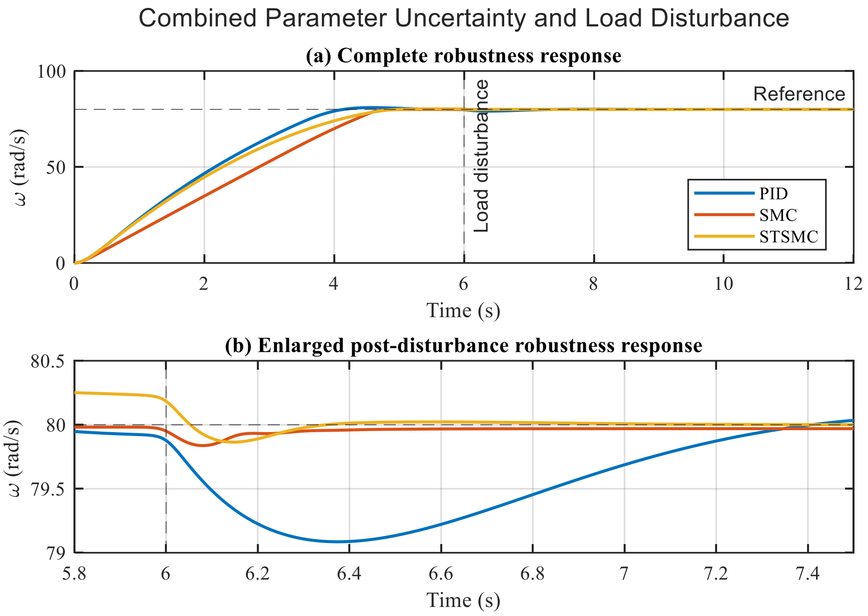

Fig. 6. Robustness comparison under combined parameter uncertainty and load-torque disturbance: (a) complete speed responses and (b) enlarged post-disturbance responses.

Table I. Nominal tracking and load-disturbance performance

Performance metric	PID	Conventional SMC	STSMC
Rise time t_r (s)	1.420	2.910	2.802
Settling time t_s (s)	1.994	3.647	3.765
Overshoot M_p (%)	1.278	0	0.520
Maximum speed deviation (rad/s)	0.86562	0.12792	0.17824
Post-disturbance IAE	0.50140	0.016906	0.13928
Post-disturbance ITAE	0.21946	0.002284	0.10691
Recovery time (s)	0.964	0.086	1.084

Table II. Chattering, control-effort, and robustness indices

Performance metric	PID	Conventional SMC	STSMC
TV(u) post-disturbance	1.8574	6.9833	1.2564
RMS(Δu) post-disturbance	0.002254	0.017210	0.002687
u_{RMS} (V), load-disturbance case	15.129	14.006	14.129
J_u, load-disturbance case	2746.7	2354.2	2395.7
IAE, uncertainty + disturbance	0.79455	0.20583	0.039963
ITAE, uncertainty + disturbance	0.54459	0.55411	0.013219
Saturation ratio, uncertainty + disturbance (%)	28.789	12.641	3.333

4.6. Comparative Discussion

The results reveal distinct performance characteristics for the three control strategies. PID favors fast nominal transients, whereas conventional SMC provides the strongest instantaneous disturbance rejection. STSMC offers a more balanced robustness-smoothness compromise by maintaining satisfactory tracking under uncertainty while substantially reducing switching activity and actuator utilization. Accordingly, the main advantage of STSMC does not lie in minimizing every individual metric, but in achieving a more practical balance among tracking performance, disturbance rejection, robustness, and control smoothness

V. CONCLUSION

This paper has established a unified comparative framework for PID, conventional sliding mode control (SMC), and super-twisting sliding mode control (STSMC) for DC motor speed regulation in the presence of load-torque disturbances, parameter uncertainties, and actuator constraints. Under the same plant model and evaluation conditions, the STSMC scheme was developed to preserve the robustness properties of sliding-mode control while mitigating the adverse effects associated with the switching action of first-order SMC.

The results demonstrate that STSMC provides a favorable balance among tracking performance, disturbance rejection, and control-signal smoothness. This finding indicates that the assessment of a robust controller should not be based solely on response speed or maximum tracking error; control effort and performance under uncertain operating conditions should also be considered. From this perspective, STSMC shows promising potential for drive systems that require consistent control performance under varying operating conditions without imposing excessive control activity on the actuator.

Within the scope of this study, the proposed approach was validated through simulations over a prescribed range of parameter variations. Future work will focus on experimental validation using a physical DC motor drive, investigation of the effects of measurement noise and sampling time, and the development of adaptive or online optimization mechanisms for the STSMC parameters to further enhance its practical implementation.

REFERENCES

[1] R. Krishnan, Electric Motor Drives: Modeling, Analysis, and Control. Upper Saddle River, NJ, USA: Prentice Hall, 2001.
[2] K. Ogata, Modern Control Engineering, 5th ed. Upper Saddle River, NJ, USA: Prentice Hall, 2010.
[3] G. F. Franklin, J. D. Powell, and A. Emami-Naeini, Feedback Control of Dynamic Systems, 8th ed. Hoboken, NJ, USA: Pearson, 2019.
[4] I. S. Okoro and C. O. Enwerem, "Robust control of a DC motor," Heliyon, vol. 6, no. 12, Art. no. e05777, Dec. 2020, doi: 10.1016/j.heliyon.2020.e05777.
[5] A. T. Alexandridis and G. C. Konstantopoulos, "Modified PI speed controllers for series-excited DC motors fed by DC/DC boost converters," Control Eng. Pract., vol. 23, pp. 14–21, Feb. 2014, doi: 10.1016/j.conengprac.2013.10.009.
[6] B. Hekimoğlu, "Optimal tuning of fractional order PID controller for DC motor speed control via chaotic atom search optimization algorithm," IEEE Access, vol. 7, pp. 38100–38114, 2019, doi: 10.1109/ACCESS.2019.2905961.
[7] V. I. Utkin, "Variable structure systems with sliding modes," IEEE Trans. Autom. Control, vol. 22, no. 2, pp. 212–222, Apr. 1977, doi: 10.1109/TAC.1977.1101446.
[8] J.-J. E. Slotine and S. S. Sastry, "Tracking control of nonlinear systems using sliding surfaces, with application to robot manipulators," Int. J. Control, vol. 38, no. 2, pp. 465–492, 1983, doi: 10.1080/00207178308933088.
[9] K. D. Young, V. I. Utkin, and U. Özgüner, "A control engineer's guide to sliding mode control," IEEE Trans. Control Syst. Technol., vol. 7, no. 3, pp. 328–342, May 1999, doi: 10.1109/87.761053.
[10] V. Utkin, J. Guldner, and J. Shi, Sliding Mode Control in Electro-Mechanical Systems, 2nd ed. Boca Raton, FL, USA: CRC Press, 2009.
[11] A. Levant, "Higher-order sliding modes, differentiation and output-feedback control," Int. J. Control, vol. 76, nos. 9–10, pp. 924–941, 2003, doi: 10.1080/0020717031000099029.
[12] A. Rauf, S. Li, R. Madonski, and J. Yang, "Continuous dynamic sliding mode control of converter-fed DC motor system with high order mismatched disturbance compensation," Trans. Inst. Meas. Control, vol. 42, no. 14, pp. 2812–2821, Oct. 2020, doi: 10.1177/0142331220933415.
[13] N. Zhou, W. Deng, X. Yang, and J. Yao, "Continuous adaptive integral recursive terminal sliding mode control for DC motors," Int. J. Control, vol. 96, no. 9, pp. 2190–2200, 2023, doi: 10.1080/00207179.2022.2086928.
[14] A. Ma'arif and A. Çakan, "Simulation and Arduino hardware implementation of DC motor control using sliding mode controller," J. Robot. Control, vol. 2, no. 6, pp. 582–587, Nov. 2021, doi: 10.18196/jrc.26140.
[15] L. Tan, J. Gao, Y. Luo, and L. Zhang, "Super-twisting sliding mode control with defined boundary layer for chattering reduction of permanent magnet linear synchronous motor," J. Mech. Sci. Technol., vol. 35, pp. 1829–1840, 2021, doi: 10.1007/s12206-021-0403-9.
[16] C. Lu and J. Yuan, "Adaptive super-twisting sliding mode control of permanent magnet synchronous motor," Complexity, vol. 2021, Art. no. 1957510, 2021, doi: 10.1155/2021/1957510.
[17] A. Choi, H. Kim, M. Hu, Y. Kim, H. Ahn, and K. You, "Super-twisting sliding mode control with SVR disturbance observer for PMSM speed regulation," Appl. Sci., vol. 12, no. 21, Art. no. 10749, 2022, doi: 10.3390/app122110749.
[18] Y.-C. Liu, S. Laghrouche, D. Depernet, A. N'Diaye, A. Djerdir, and M. Cirrincione, "Super-twisting sliding-mode observer-based model reference adaptive speed control for PMSM drives," J. Franklin Inst., vol. 360, no. 2, pp. 985–1004, 2023, doi: 10.1016/j.jfranklin.2022.12.014.
[19] K. Zhao, N. Jia, J. She, W. Dai, R. Zhou, W. Liu, and X. Li, "Robust model-free super-twisting sliding-mode control method based on extended sliding-mode disturbance observer for PMSM drive system," Control Eng. Pract., vol. 139, Art. no. 105657, Oct. 2023, doi: 10.1016/j.conengprac.2023.105657.